

Supporting Information

Grain-boundary engineering of Ni-rich cathodes prolongs cycle life of Li-ion batteries

Lele Cai¹, Qiang Han², Huawei Zhu¹, Haifeng Yu¹, Yanjie Hu¹, Hao Jiang^{1,2,*}

¹ Shanghai Engineering Research Center of Hierarchical Nanomaterials, School of Materials Science and Engineering, East China University of Science and Technology, Shanghai 200237, China

² Key Laboratory for Ultrafine Materials of Ministry of Education, School of Chemical Engineering, East China University of Science and Technology, Shanghai 200237, China

* E-mail: jianghao@ecust.edu.cn (Prof. H. Jiang)

Tel.: +86-21-64250949, Fax: +86-21-64250624

1. Supplementary Note.

1.1 Material characterization

The X-ray diffraction (XRD, Bruker D8 Advance, Cu K α radiation) was used to probe the crystal structure of all the cathodes. The Rietveld refinement was employed to fit the lattice parameters. The Field emission scanning electron microscopy (FESEM, Hitachi, S-4800) and the transmission electron microscopy (TEM, FEI Talos F200X) with an X-ray energy-dispersive spectrometer (EDS) was used to study the morphologies, microstructure and elemental distribution of the samples. The focused ion beam etching technique was performed to prepare the TEM sample. The structural stability of samples was analyzed by in-situ high-temperature X-ray diffraction (HT-XRD) within the temperature range of 30-500 °C. The gas evolution was measured by in-situ differential electrochemical mass spectrometry (DEMS) with delithiated cathode (4.3 V) at 55 °C.

1.2 Electrochemical measurements

The slurry was made by blending 80wt.% active material with 10wt.% Super-P and 10wt.% poly (vinylidene fluoride) in a suitable amount of N-methyl-2-pyrrolidone solvent. The aluminum foil was then coated with a slurry and vacuum dried to prepare single-sided coated electrodes (loading mass: $\sim 2.0 \text{ mg cm}^{-2}$). The glovebox with filled argon was used to assemble the 2016 coin-type cells. The negative electrode was lithium metal, the separator was polypropylene membrane (Celgard 2400) and the electrolyte was 1.2 M LiPF₆ (battery level) in ethylene carbonate: ethyl methyl carbonate (3:7 by volume) with 2 wt.% vinylene carbonates. The pouch cells were assembled with two samples as cathodes and the commercial graphite as anode (cathode loading mass: $\sim 12.0 \text{ mg cm}^{-2}$, N/P = 1.1). The cathode was stacked with anode and membrane. Subsequently, the pouch cell was obtained by injecting electrolyte into dry cells packed with aluminum plastic film. The galvanostatic charge and discharge tests were conducted by using the LANDCT2001A battery test system

at 25 and 55 °C, the value of 1C was 180 mAh g⁻¹. The galvanostatic intermittent titration technique (GITT) test was carried out in LANDCT2001A test system with 1 h relaxation time after charging for 10 min at 0.1 C. The cyclic voltammetry curves (CV) and electrochemical impedance spectroscopy (EIS) experiment was conducted in Autolab PGSTAT302N electrochemical workstation with a range of 100 kHz to 0.01 Hz.

1.3 The testing process and calculation equation of GITT measurement

Before the GITT measurement, the cells were firstly galvanostatic charge/discharged for 3 cycles. GITT measurements were performed by charging/discharging the fully activated cells at a constant current (0.1C) for an interval of 10 min followed by an open circuit stand for 1 h to allow the cell voltage to relax to its quasi-equilibrium state. The change in the steady-state voltage ΔE_s is obtained by subtracting the original voltage (E_0) from the steady-state voltage (E_s). The cell voltage increases during the current flux and the total change of cell voltage ΔE_τ can be obtained by calculating the voltage drop. Meanwhile, the process of the chemical diffusion is assumed to obey Fick's second law of diffusion. With a series of simplifications, for sufficient time interval ($\tau \ll L^2/D_{Li^+}$), the equation of D_{Li^+} can be written as (Equation 2):

$$D_{Li^+} = \frac{4L^2}{\pi\tau} \left(\frac{\Delta E_s}{\Delta E_\tau} \right)^2 \left(\tau \ll \frac{L^2}{D_{Li^+}} \right)$$

where ΔE_s is the value of subtracting the original voltage (E_0) from the steady-state voltage (E_s). ΔE_τ is the change in the total temporary potential during the application of current in τ , L is the thickness of the electrode.^[1,2]

2. Supporting Figures

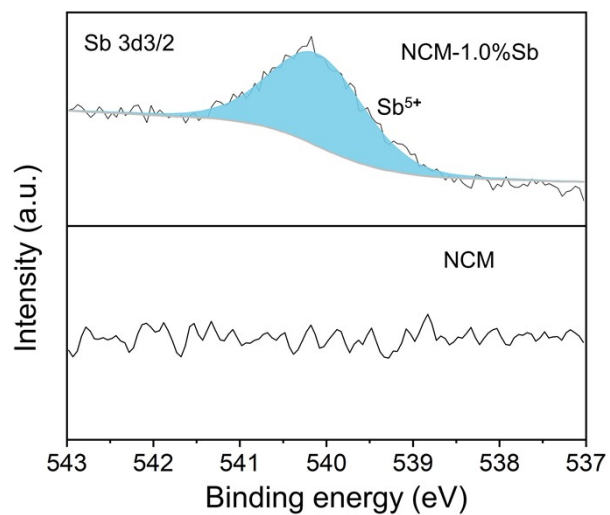


Fig. S1 Sb 3d XPS spectra of the pristine NCM and NCM-1.0%Sb.

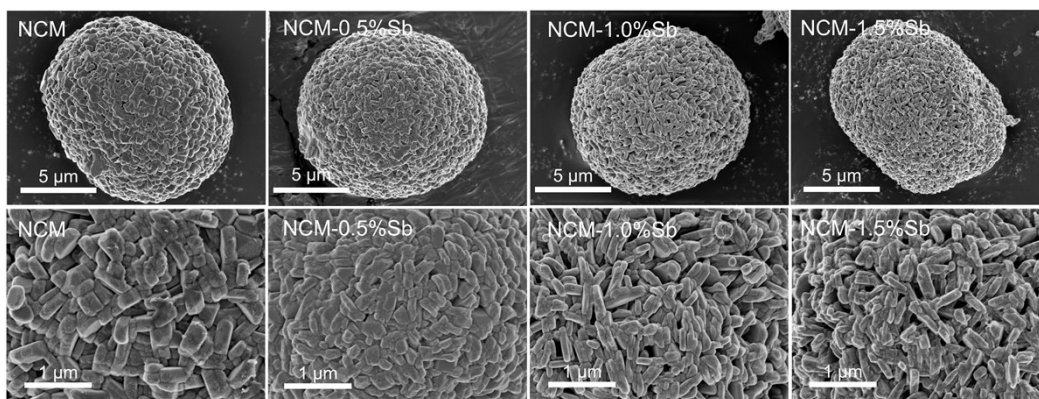


Fig. S2 Low/High-magnification SEM image of the NCM, NCM-0.5%Sb, NCM-1.0%Sb and NCM-1.5%Sb cathodes.

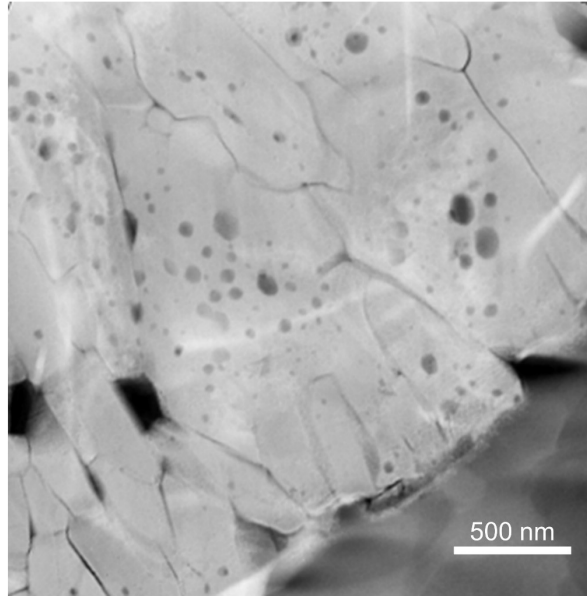


Fig. S3 Cross-section STEM-HAADF image of the pristine NCM.

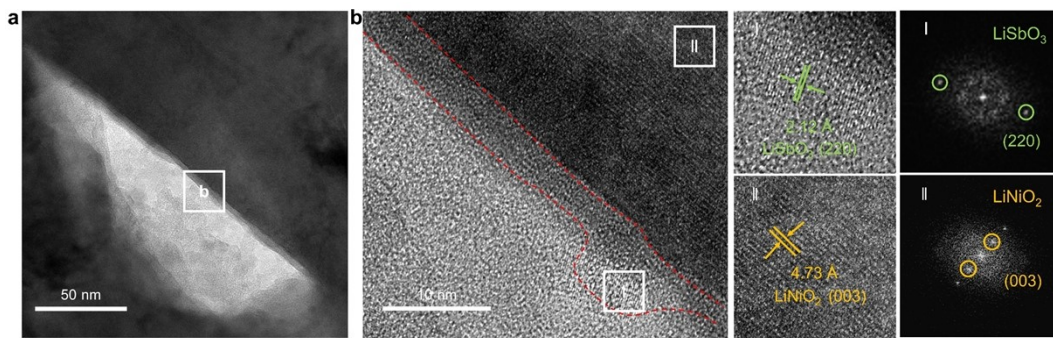


Fig. S4 (a) TEM, (b) high-resolution TEM images and corresponding fast Fourier transform (FFT) for the NCM-1.0%Sb.

Notes: The TEM image of NCM-1.0%Sb is also provided in Figure S4a. Zooming in further discloses a uniform LiSbO_3 coating layer, as shown in Figure S4b. The lattice spacing of 2.12 Å (region I) is indexed to the (220) plane of the LiSbO_3 (JCPDS 43-0128) while the lattice spacing of 4.73 Å (region II) is attributed to the (003) plane of the LiNiO_2 (JCPDS 09-0063).

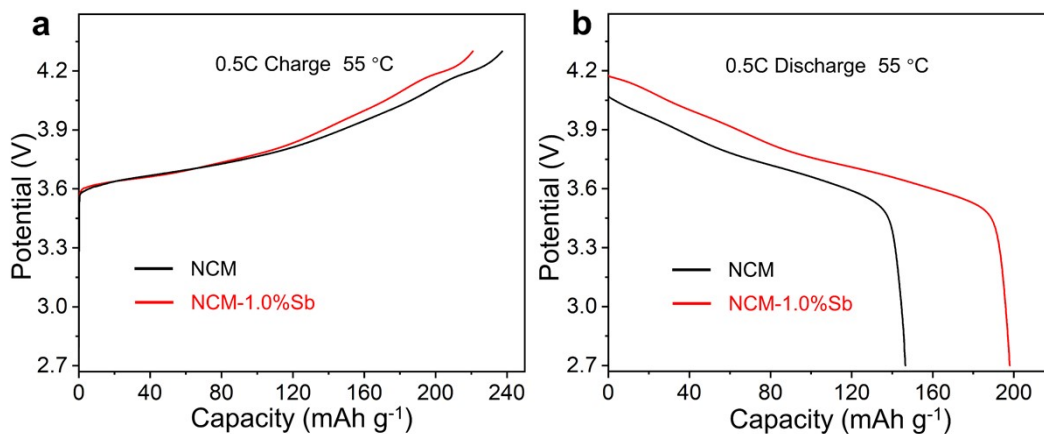


Fig. S5 Self-discharge test of NCM and NCM-1.0%Sb at 55 °C: (a) the charge curve at 0.5C, (b) the discharge curve after resting.

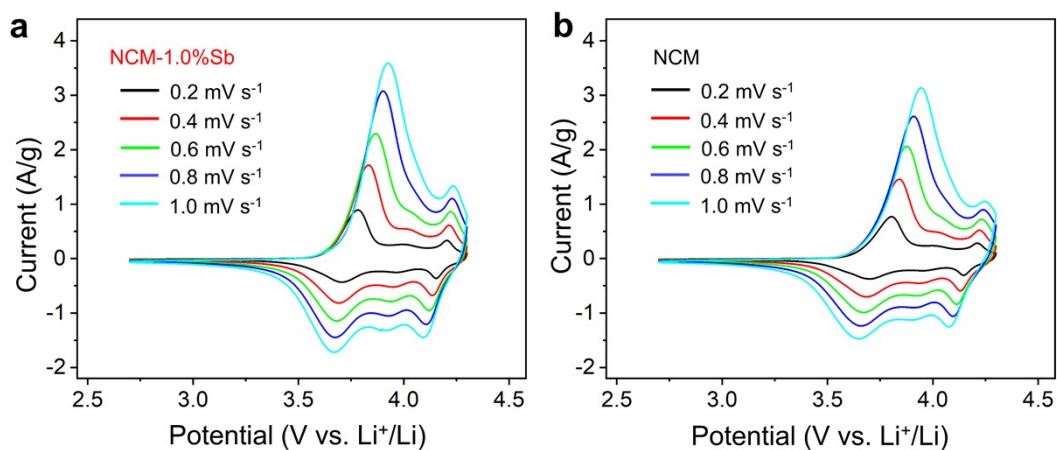


Fig. S6 CV curves of (a) NCM-1.0%Sb and (b) NCM from 0.2 to 1.0 mV s⁻¹.

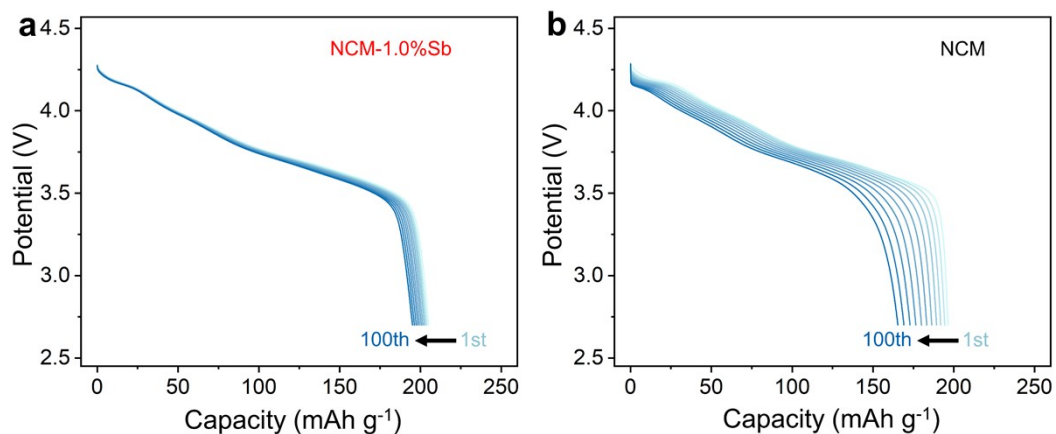


Fig. S7 discharge curves of NCM-1.0%Sb and NCM at 1 C and 55 °C.

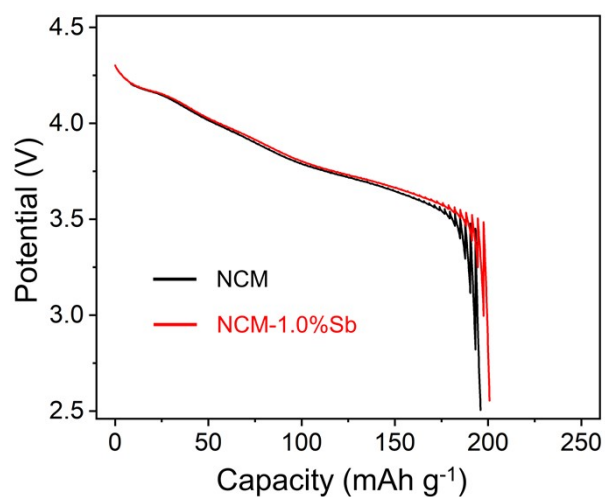


Fig. S8 GITT of discharge curves for NCM-1.0%Sb and pristine NCM.

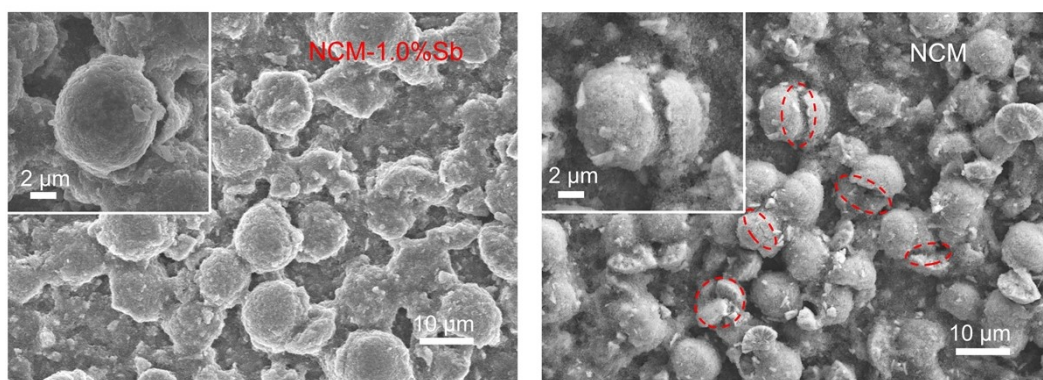


Fig. S9 SEM images after 100 cycles at 1C and 55 °C for (a) NCM-1.0%Sb and (b) NCM.

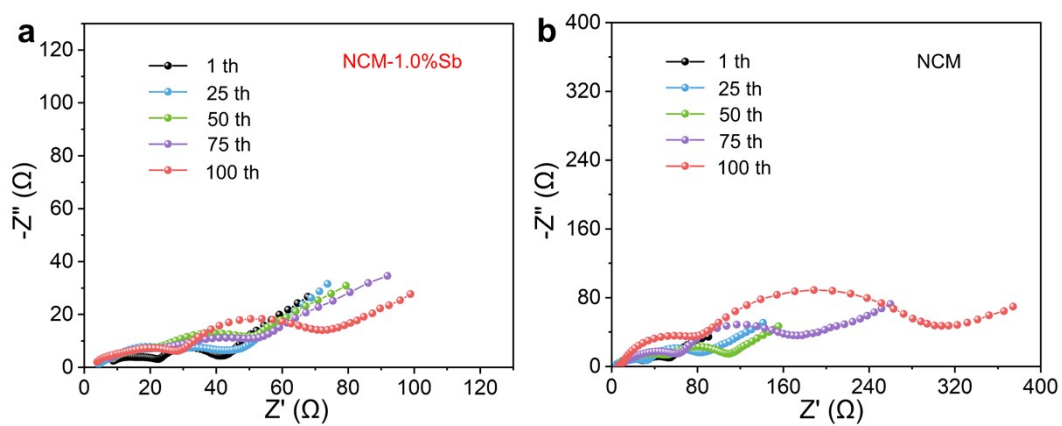


Fig. S10 Nyquist plots after different cycles of (a) NCM-1.0%Sb and (b) NCM.

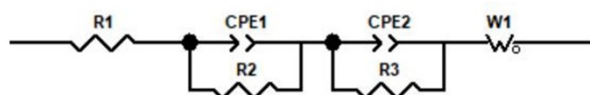


Fig. S11 The corresponding equivalent circuit for the impedance spectra.

Part 2 Supporting Tables

Table S1 The detailed chemical composition of all synthesized cathode materials

Samples	Chemical Composition (at%)			
	Ni	Co	Mn	Sb
NCM-0.5%Sb	82.49	10.91	6.1	0.50
NCM-1.0%Sb	82.13	10.91	6.0	0.96
NCM-1.5%Sb	81.68	10.90	6.0	1.42
NCM	82.88	10.92	6.2	-

Table S2 The results of XRD Rietveld refinement for NCM-1.0%Sb and NCM

Samples	a (Å)	c (Å)	V (Å ³)	R _{wp}	x ²
NCM-0.5%Sb	2.87098	14.19155	101.303	6.14	1.127
NCM-1.0%Sb	2.87111	14.20225	101.388	5.95	1.166
NCM-1.5%Sb	2.87138	14.21234	101.479	5.88	1.118
NCM83	2.87017	14.19053	101.238	6.11	1.256

Table S3 The R_{sf} and R_{ct} data obtained from the Nyquist plots in different cycle numbers

Samples	NCM-1.0%Sb		NCM	
	R _{sf} (Ω)	R _{ct} (Ω)	R _{sf} (Ω)	R _{ct} (Ω)
1 st	23.55	28.46	32.83	39.48
25 th	26.67	39.24	44.89	60.46
50 th	28.31	46.11	67.86	71.50
75 th	32.96	50.94	81.11	129.85
100 th	39.03	52.57	99.21	247.91

References

1. H. Yu, H. Zhu, H. Jiang, X. Su, Y. Hu, H. Jiang and C. Li, *Nati. Sci. Rev.*, 2023, **10**, nwac166.

2. H. Yu, Y. Cao, L. Chen, Y. Hu, X. Duan, S. Dai, C. Li and H. Jiang, *Nat. Commun.*, 2021, **12**, 4564.